



Performance Analysis of Three-sides Concave Dimple Shape Roughened Solar Air Heater

Vikash Kumar^{*1}, Laljee Prasad²

¹Department of Mechanical Engineering, National Institute of Technology Jamshedpur, Adityapur,
District Seraikela Kharsawan, Jamshedpur, Jharkhand 831014, India

e-mail: Vikash.rsme004@nitjsr.ac.in

²Department of Mechanical Engineering, National Institute of Technology Jamshedpur, Adityapur,
District Seraikela Kharsawan, Jamshedpur, Jharkhand 831014, India

e-mail: Lalprch1@rediffmail.com

Cite as: Kumar, V., Prasad, L., Performance Analysis of Three-sides Concave Dimple Shape Roughened Solar Air Heater, J. sustain. dev. energy water environ. syst., 6(4), pp 631-648, 2018, DOI: <https://doi.org/10.13044/j.sdewes.d6.0211>

ABSTRACT

Three-sides artificially roughened solar air heaters perform better than one-side roughened ones under identical operating conditions. The present paper is an outcome of the experimental investigations conducted upon three- and one-side concave dimple roughened ducts. The present investigation is carried out under the mass flow rate range (0.0060-0.0250) kg/s, relative roughness pitch (p/e) 8-16 and relative roughness height (e/D_h) 0.018-0.045. Thermal performance characteristics of three-sides and one-side roughened duct has been analyzed, compared and validated. The variation in plate temperature along the test length of the roughened duct has an appreciable impact on the heat transfer from the plate to the underside flowing air. The collector's surface temperature is found to be 21% lower in the three-sides than the one-side roughened duct. Plate temperature excess for both three-sides and one-side roughened duct has been analyzed and compared. The plate temperature excess range for three-sides roughened duct is significantly lower (12.5-28.5 °C) compared to one-side roughened duct (17.5-35.5 °C). The augmentation in fluid (air) temperature flowing under three-sides concave dimple roughened duct is found to be 34.87% more than one-side roughened duct. The augmentation in thermal performance due to the provision of roughness geometry in the form of concave dimple shape on the three-sides over one-side roughened duct is found to be 39-56% for varying p/e and 44-51% for varying e/D_h depending upon the operational mass flow rate of air and roughness geometry. The maximum thermal efficiency is obtained at relative roughness pitch of 12 and relative roughness height of 0.036. The results for efficiency ratio along with parametric variation influence on performance of the roughened ducts have also been discussed in detail.

KEYWORDS

Three-side roughened duct, One-side roughened duct, Relative roughness pitch, Relative roughness height, Thermal performance, Plate temperature excess.

INTRODUCTION

The thermal efficiency of non-roughened flat plate solar collector is low compared to solar water heater due to the fact that convective heat transfer coefficient and thermal

* Corresponding author

capacity of air is low [1]. As a result, there is minimum transfer of heat from the collector surface to the under-flowing air resulting in higher collector temperature and lower thermal efficiency. Higher plate temperature leads to higher heat loss to the surroundings [2]. Numerous researchers have worked on methods that would result in an appreciable augmentation in the heat transfer rate from the absorber surface to the under-flowing fluid (air). This can be done in multiple ways like increasing the surface area of the collector or by providing artificial roughness on the air side of the collector surface [3-6]. Providing artificial roughness is an efficacious technique to enhance the heat transfer coefficient and hence thermal performance [7]. Artificial roughness of different geometries under varying geometrical parameters has been used by various researchers that have yielded better results in terms of heat transfer and thermal performance [8-9]. Figures 1 and 2 show different roughness geometries under varying orientation used by various researchers.

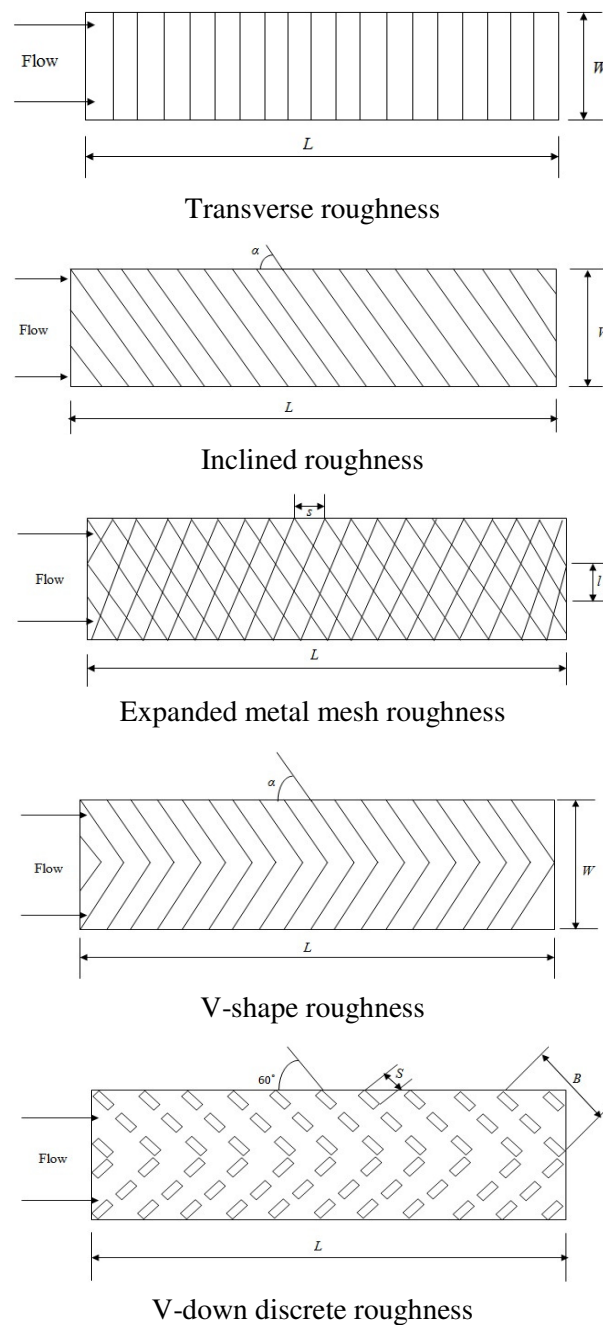


Figure 1. Various roughness geometries used by researchers

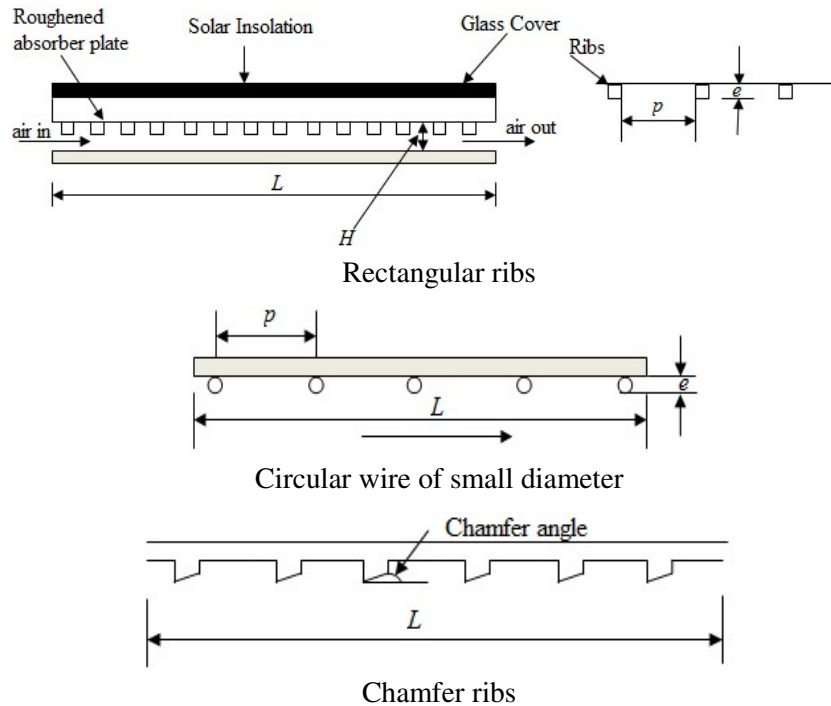


Figure 2. Orientation of various roughness geometries

A brief description of different flow patterns due to the provision of artificial roughness under different roughness geometries is presented in Figure 3. Artificial roughness applied to the absorber plate may be of rectangular, circular cross-section, dimples, protrusions, fins, wedge, chamfered, discrete ribs, etc. For circular ribs or rectangular wire of small diameter aligned parallel or transverse to the flow direction, it has been discovered that flow gets separated near the ribs and re-adheres in the vicinity of inner rib space at a p/e value of 7 or more [10]. The laminar sub-layer lying near to the ribs get destroyed completely at the reattachment point resulting in enhanced heat transfer coefficient in the vicinity of roughness provided. As soon as the reattachment point is reached, the boundary layer redevelops at downstream flow resulting in less heat transfer in the presence of roughened elements (wire or ribs) that extends up to the beginning of next re-attachment point [11].

For a collector having chamfered ribs aligned positively at relative roughness pitch $p/e \leq 5$, strenuous eddy shedding is observed compared to square or negatively chamfered roughened collector. Reattachment effect in the case of chamfered ribs is seen at relative roughness pitch p/e as low as 5 thereby reducing the recirculating flow region and laminar sub-layer thickness [11]. The literature reveals that heat transfer augmentation is more when the roughness elements are aligned at inclination or are v-shaped roughened instead of transverse roughness pattern [12]. When the ribs are in v-pattern or inclined to the flow, secondary flow (flow of heated air in contact with roughness element) is induced due to the inclination of ribs as shown in Figure 3. The heated air tends to move towards the side walls in case of inclined ribs [13]. In case of v-up or v-down pattern, the heated air moves towards the side walls and centre of ribs, respectively. Thus the entire absorber plate is exposed to the primary air (axially flowing air) which is at comparatively lower temperature with respect to the secondary air, resulting in more heat transfer from the collector surface to the under-flowing air [14]. Temperature along the central axis of the flowing air is higher in the case of v-down roughened collector than v-up rib arrangement because secondary flow moving towards the central axis gets intermingled with the axial flow (primary flow) causing additional turbulence resulting in higher heat transfer [15-16].

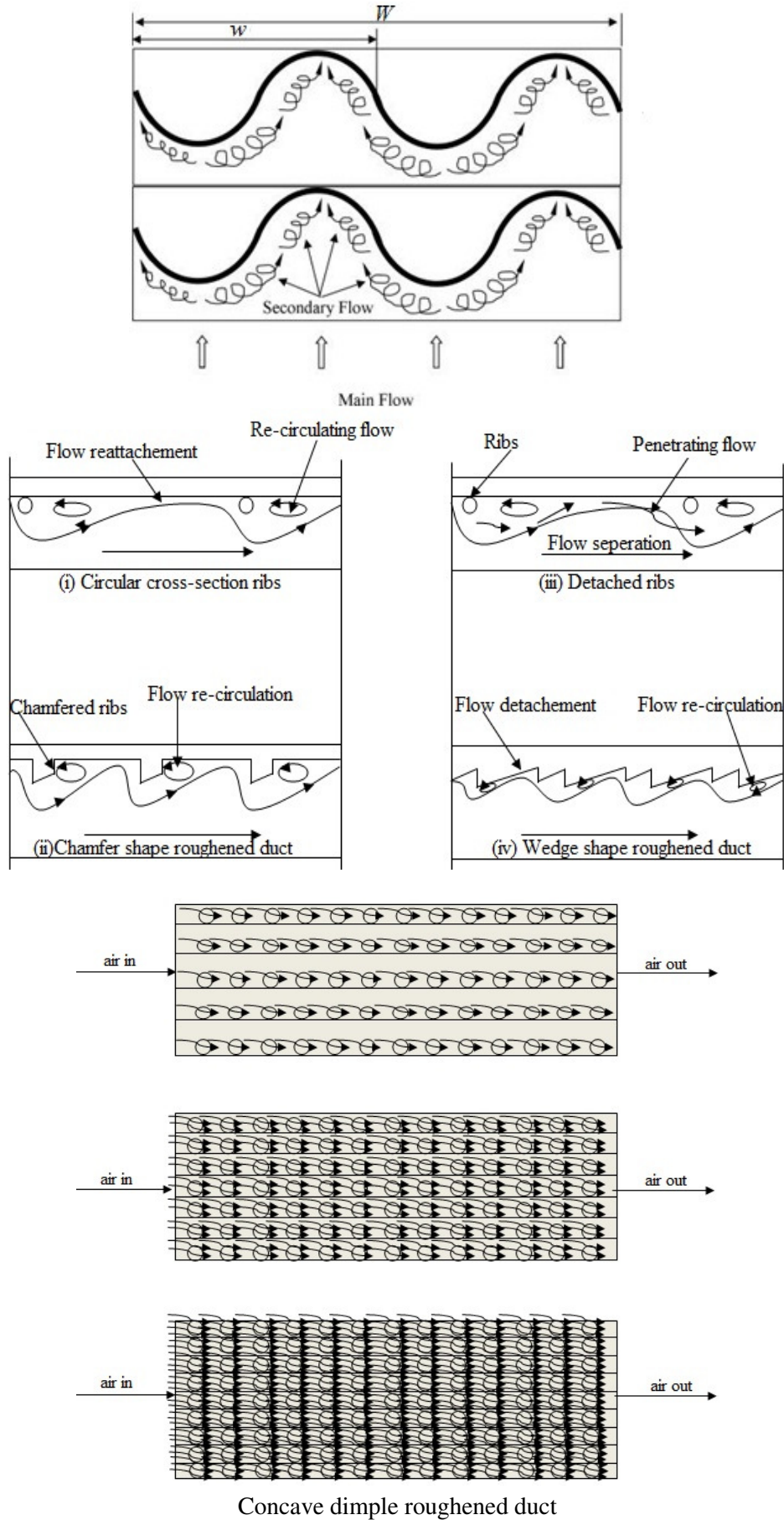


Figure 3. Flow pattern in various shapes artificially roughened ducts (only top side roughened)

Solar air heater roughened with crossed wires mesh as in Saini and Saini [17], the flow of air under expanded metal mesh was quite complex. It was noticed that the heat transfer augmentation was not much for $0 < p/e \leq 7$ due to the fact that flow was dominated by vortex formation. For the plate configuration of $7 < p/e \leq 25$, there is an appreciable increase in heat transfer augmentation because of presence of re-attachment effect and secondary flow.

The heat transfer augmentation due to provision of artificial roughness is often followed with the pressure drop enhancement across the duct. Pressure drop enhancement is caused mainly due to increase in frictional resistance offered by the roughened element to the flow. The literature revealed above indicates that there is an appreciable augmentation in both heat transfer and friction factor, as both have a strong dependence on flow and geometrical parameters. Optimal conditions were defined for artificially roughened solar heater, which would give better performance under minimum loss for a given flow and geometrical conditions. Prasad *et al.* [18] carried out investigations on three-sides artificially roughened solar air heater and concluded that

roughness Reynolds number, $e_{\text{opt}}^+ = \frac{e}{D} \sqrt{\frac{f_r}{2}}$. $Re = 23$ always corresponds to the optimal thermohydraulic performance under varying set of values for p/e , e/D_h and Re used separately or combined. Hence, roughness should be provided such that maximum thermal enhancement is achieved at minimum pressure drop penalty [19].

It is clearly depicted in the literature of artificially roughened solar air heater that most of the roughness provided is in the form of wire, ribs, wire mesh, expanded metal mesh, fins, etc. All these roughness geometries would require a complex manufacturing process and also contribute to the extra weight of the absorber plate. Providing roughness in the form of dimples is considered as effective roughness geometry as it is easy to fabricate, especially if dimples to be formed are of spherical indentation and concave in nature [20].

Most of the studies in the literature have remained limited to only one side of the absorber plate (top side) while the bottom and side walls do not participate in heat transfer process. If roughness is provided to the two side walls, they can participate in the heat transfer augmentation process resulting in an appreciable enhancement in heat transfer.

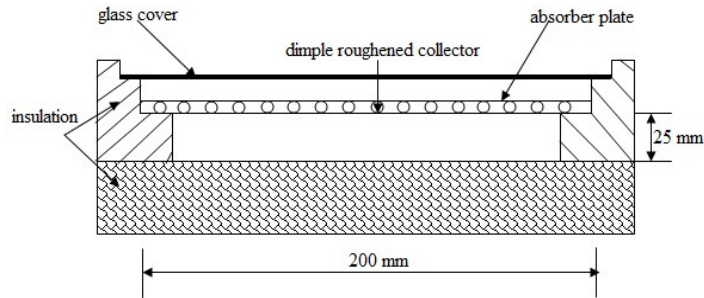
Keeping in mind the above works, the present investigation is based on three-sides (top and sides) artificially roughened solar air heaters, embossed with concave dimples of varying height and pitch as roughness element [21-22]. The objectives of the present work are:

- To develop such solar air heaters and carry out experiments under actual outdoor conditions and collect various sets of data for one-side as well as three-sides roughened solar air heaters;
- To reduce the experimental data to work out the thermal efficiency results in such solar air heaters and validate them with available data;
- To discuss the effects of roughness and flow parameters on thermal performance of such solar air heaters.

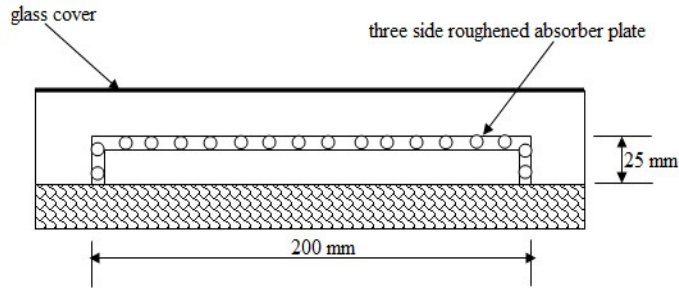
EXPERIMENTAL SET-UP

The test setup used for experimentation in the present work has been fabricated as per the guidelines of ASHRAE Standard for testing roughened solar collectors under actual outdoor conditions using open loop system [23].

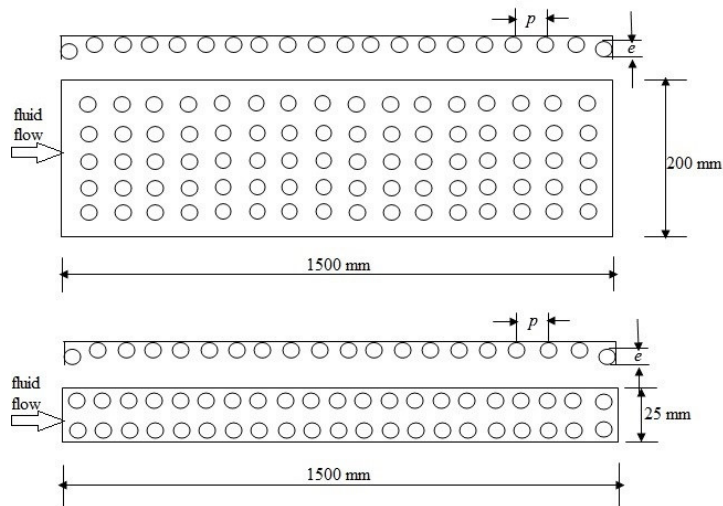
Figure 4 shows the actual and schematic layout of the experimental setup developed with quality plywood and wooden boards. The setup is accommodated with three ducts parallel to each other namely A, B and C as shown in Figure 4. The present investigation employs the duct A and C containing one- and three-sides roughened absorber plates respectively.



One side roughened duct with two sides insulation



Three sides roughened duct with one side insulation



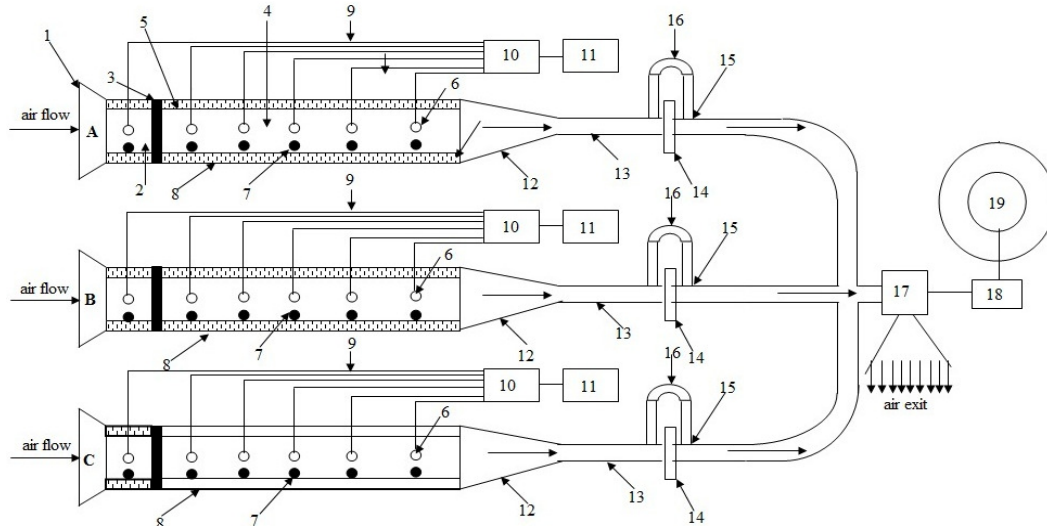
Top and side view of three sides roughened absorber plate



Photograph of three- and one-side roughened absorber plate



Photograph of the experimental set-up



Line diagram of the experimental set-up

- | | |
|---|------------------------|
| 1. Trapezoidal shaped air inlet | 10. Selector switch |
| 2. Non-roughened duct section | 11. Digital voltmeter |
| 3. Insulation between entry and test length | 12. Converging section |
| 4. Roughened duct section | 13. Cylindrical pipe |
| 5. Insulation | 14. Orifice-plate |
| 6. Thermocouple | 15. Flange couplings |
| 7. Thermometer | 16. U-tube manometer |
| 8. Glass covers | 17. Blower |
| 9. Copper wire | 18. Motor |
| | 19. Variac |

Figure 4. Actual and schematic diagram of experimental set-up of roughened duct

The test setup is, 2.13 m long, 0.7 m wide and 50 mm high. Three ducts each of width 200 mm are formed to accommodate the absorber plates. Each duct is 2,130 mm long out of which 1,500 mm length is the test length and 500 mm is entry length. Only the test length is instrumented and the remaining 500 mm entry length serves the purpose of flow stabilization [24]. For one-side roughened duct, roughness is provided at the bottom (air flow side) of the absorber plate, two sides are insulated, top side is provided with 4 mm thick glass cover and the bottom is insulated by means of the wooden part of the duct. For three-sides roughened duct, roughness is provided on the three sides, i.e., one top and two side walls of the absorber plate. Three-sides roughened duct contains three side glass covers (250 mm × 50 mm × 50 mm) and bottom side insulation. The two ducts used in the experimental setup are similar in all terms of dimensions and orientation so that heat transfer and thermal performance characteristics can be directly compared. The sun facing sides of the absorber plates are painted with black colour of high absorptivity to absorb maximum possible incident solar radiation. All the joints were perfectly sealed using lightly moistened putty and m-seal to ensure an air-tight setup. Calibrated copper constantan thermocouples are used to measure plate temperatures as shown in Figure 5. Eighteen thermocouples were used to measure the plate temperature whose output is given by a digital voltmeter assembled in the setup. Six out of eighteen thermocouples were placed on the top of one side roughened duct and 12 thermocouples were placed on three sides roughened (six on top and six on side walls) absorber plate. Digital thermometer was used to measure the air temperature flowing inside the ducts. Before starting the experiment, it was ensured that all the experimental components were working properly. The blower was switched on at 06:00 hour in the morning and the readings were taken from 10:00 hour, four hours after exposure of the absorber plate to

solar radiation and to achieve stagnation gap between the absorber plate and glass cover. The desired flow rate of air through the duct was regulated using an auto variac. The readings were taken at intervals of 15 min from 10:00 to 15:00 hours for six clear sky days at six different mass flow rates for each set of the absorber plate.

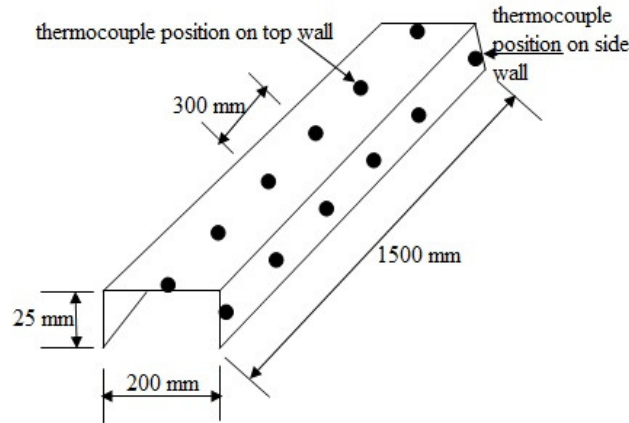


Figure 5. Thermocouple positions located on top and side walls of the absorber plate

The geometrical and roughness parameters of the experimental setup and the experimental outdoor conditions, like mass flow rate, ambient temperature, wind speed, global radiation, etc. used during experimentation are mentioned in Table 1.

Table 1. Range of flow and geometrical parameters

S. No.	Name of parameter	Symbolic representation	Range of operating parameter
1.	Flow rate of air	\dot{m}	0.0060-0.0250 kg/s
2.	Relative roughness pitch	p/e	8-16
3.	Relative roughness height	e/D_h	0.018-0.045
4.	Ambient temperature	T_∞	24-44 °C
5.	Insolation	I	720-960 W/m ²
6.	Wind speed	v_∞	0.5-3.5 m/s

DATA REDUCTION

The useful heat gain from the heated absorber plate to the underside flowing fluid (air) can be evaluated using the values air inlet temperature (T_i) and air outlet temperature (T_o). Thus:

$$Q_u = \dot{m}C_p (T_o - T_i) \quad (1)$$

where \dot{m} is mass flow rate of air and C_p is specific heat capacity of air flowing through the roughened duct.

The mass flow rate prevailing through the roughened duct is determined using pressure drop (ΔP_o) across the orifice plate [25]:

$$\dot{m} = C_d A_o \left[\frac{2\rho_a \Delta P_o \sin \theta}{1 - \beta^4} \right]^{0.5} \quad (2)$$

The mean temperature of the absorber plate has been calculated based on readings of digital voltmeter that reads the output of thermocouples placed on 'n' different locations of the absorber plate as:

$$T_{pm} = \frac{1}{L} \sum_{i=1}^n T_{pi} \times L_i \quad (3)$$

where L is test length of collector.

The mean temperature of fluid (air in the present case) is simply the arithmetic mean of air inlet and outlet temperatures and hence calculated as:

$$T_{im} = \frac{1}{2} (T_i + T_o) \quad (4)$$

D_h is the hydraulic diameter of the duct and is evaluated as:

$$D_h = \frac{4WH}{[2(W + H)]} \quad (5)$$

where L , H and W are length, height and width of the roughened duct respectively.

The thermal efficiency of artificially roughened solar air heater is defined as the ratio of useful heat gain (Q_u) per unit area of the absorber plate to the incident thermal radiation upon it and is calculated as:

$$\eta = \frac{Q_u}{IA_p} \quad (6)$$

where Q_u is useful heat gain, I is incident thermal radiation and A_p is aperture area of collector.

The pressure drop was determined for the test length 1,500 mm using Darcy Weisbach equation:

$$\Delta p = \frac{4f\rho LV^2}{2D_h} \quad (7)$$

where f is co-efficient of friction, ρ is density of air, L is length of the absorber plate, V is velocity of flow and D_h is hydraulic diameter.

MEASUREMENT UNCERTAINTY

The experimental data recorded during investigation often differ from the actual data due to a lot of unaccountable factors while performing experiments. This deviation of the recorded data from actual data is called as uncertainty. The uncertainty prevailing in the measurement of various parameters has been calculated following a procedure suggested by Klein and McClintock [26].

The uncertainty analysis has been carried out for the entire set of parameters investigated within the operating range and the uncertainty variation of various parameters obtained is presented in Table 2.

Table 2. Uncertainty range in measurement of operating parameter

S. No.	Operating parameters	Uncertainty range [%]
1.	Mass flow rate of air	1.43-2.76
2.	Useful heat gain by air	1.85-3.10
3.	Thermal performance of roughened duct	2.57-4.20

RESULTS AND DISCUSSION

Rigorous experimentation has been performed and data for both three-sides and one-side roughened ducts have been recorded simultaneously at different mass flow rates. The test run for one set of absorber plates was six clear sky days as each day had a fixed mass flow rate. Following parameters were measured during each of those days [27]:

- Pressure drop across orifice meter (ΔP_o);
- Pressure drop across the duct (ΔP_d);
- Temperature of the collector (T_p);
- Temperature of the air in the roughened duct (T_f);
- Ambient air temperature (T_∞);
- Solar radiation intensity (I).

Variation in ambient conditions

Figure 6 typically shows the variation of solar radiation intensity [W/m^2] and ambient temperature [$^\circ C$] on a clear sky day with respect to local time [hh:mm] during experimental period (10:00 to 15:00 hours). It can be seen that as the day progresses, the intensity of solar radiation increases remarkably up to 12:30 hours after which it decreases. Ambient temperature increases monotonously as shown in Figure 6. The maximum value of solar intensity and ambient temperature was recorded at 13:30 hours respectively as $920.97 W/m^2$ and $41.73 ^\circ C$.

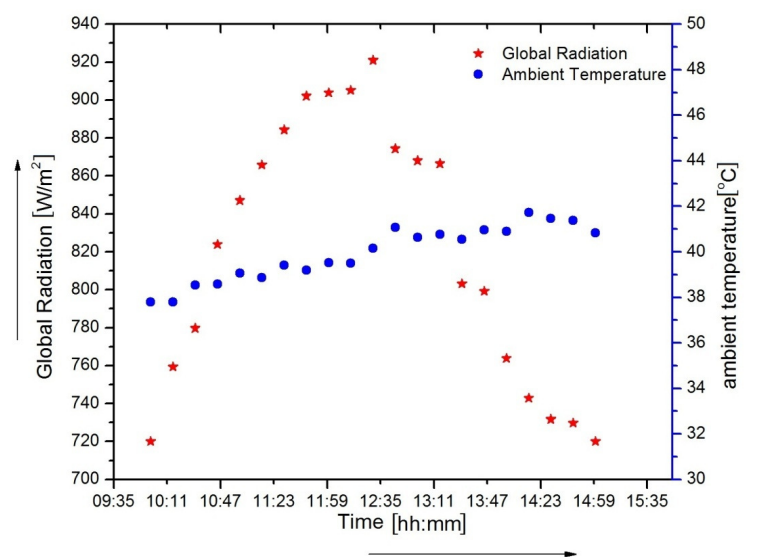


Figure 6. Variation of global intensity and ambient temperature with time

Validation

The thermal efficiency values for three-sides and one-side roughened duct are shown in Figure 7. The present experimental values of thermal efficiency for one-side roughened duct was found to be in range and compared well with a similar duct model of Saini and Verma [28]. Three-sides dimple roughened solar air heater data is not available for direct comparison. Since one-side dimple roughened solar air heater data compare well, the results for three-sides concave dimple roughened ones are worth to be valid and hence have been utilized further. The percentage mean deviation of thermal efficiency for one- side roughened duct was found to be $\pm 3.6\%$. The augmentation in the value of thermal efficiency for three-sides roughened duct when compared to one-side roughened duct was found to be in the range of 28-41%.

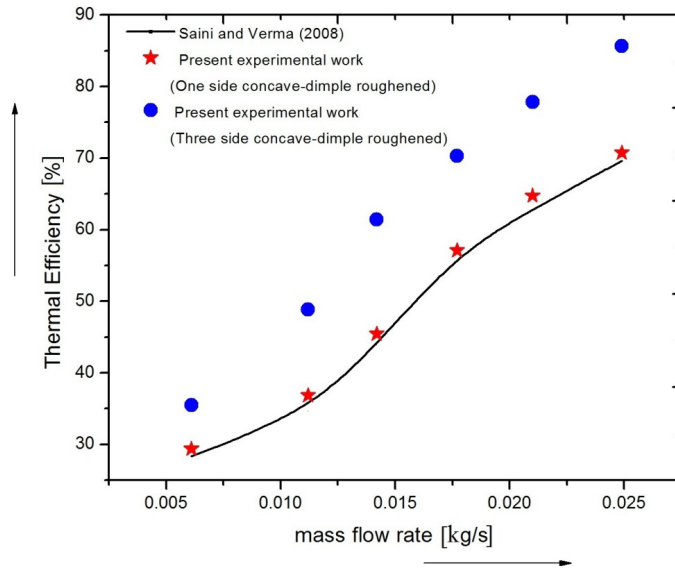


Figure 7. Experimental values of thermal efficiency for three- and one-side roughened ducts

Plate and air temperature along test length

Figure 8 shows the variation in air and plate temperature for three-sides and one-side artificially roughened collector along the test length. It can be observed that the rise in air temperature for three-sides roughened duct is more than the temperature rise for one-side roughened duct along the test length of the collector. Meanwhile, for plate temperature, one-side roughened duct experiences more temperature rise than three-sides roughened duct due to minimal heat transfer to the under flowing fluid (air) along the test length of the collector.

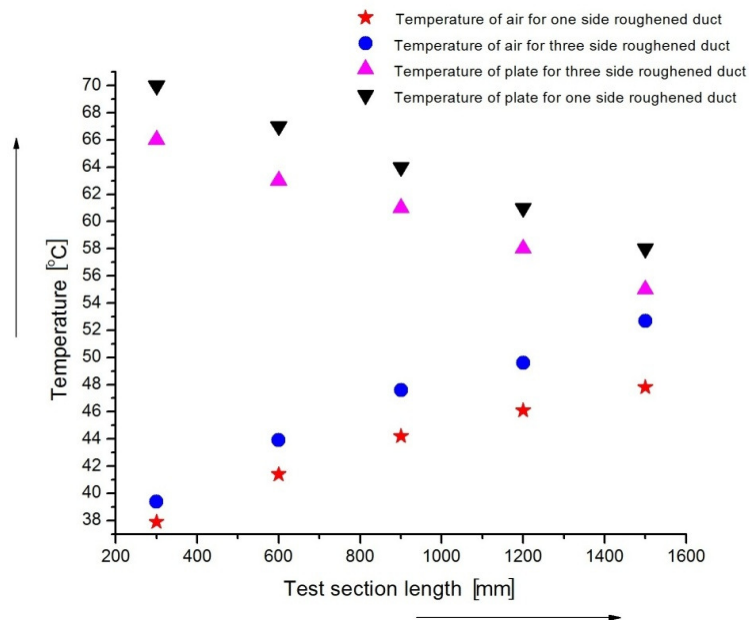


Figure 8. Variation in plate temperature along test length

Plate excess temperature for one- and three-sides roughened ducts

The mass flow rate affects the thermal performance of artificially roughened solar air heater to a great extent. Figures 9a and 9b shows the plate temperature excess for one side and three sides roughened duct respectively. The plate temperature excess (difference between plate mean temperature and ambient temperature) of both three sides and one

side roughened duct decreases with an increase in flow rate of air. Providing artificial roughness on the collector's surface results in an increase of convective heat transfer coefficient of the flowing air under the roughened duct with the increasing mass flow rate. This is attributed to an increase in useful heat gain, consequently reducing plate temperature, which in turn reduces the heat loss from the collector to the nearby surroundings. The effect of increased convective heat transfer coefficient on the plate temperature can be seen in Figures 9a and 9b where the plate temperature excess has been plotted against increasing mass flow rate. The plate temperature excess range for three-sides roughened duct is convincingly lower, 12.5-28.5 °C than one-side roughened duct which is 17.5-35.5 °C. Hence, three sides roughened duct having a high rate of heat transfer operates at lower plate temperature resulting in higher thermal efficiency due to reduction in heat loss from the absorber plate.

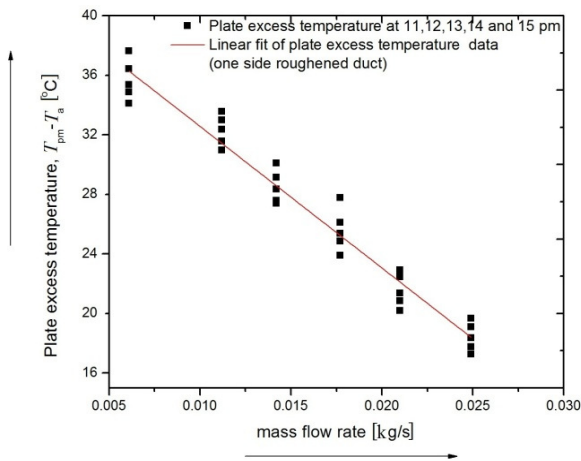


Figure 9a. Plate temperature excess vs. \dot{m} (one-side roughened duct)

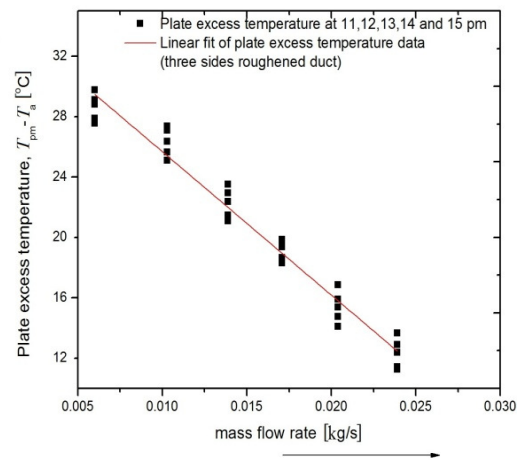


Figure 9b. Plate temperature excess vs. \dot{m} (three-sides roughened duct)

Thermal performance

A comprehensive thermal performance study of concave dimple roughened solar air heaters have been carried out for a wide range of flow and geometrical parameters. The results are shown as thermal efficiency versus mass flow rate. The mass flow rate (\dot{m}) has been varied from 0.0060 kg/s to 0.0250 kg/s. The relative roughness pitch (p/e) has been varied from 8 to 16. The relative roughness height (e/D_h) has been varied from 0.018 to 0.045.

It can be seen from Figures 10 and 11 that with an increasing mass flow rate, the thermal efficiency of both three-sides and one-side roughened duct increases. Three-sides roughened solar air heater is significantly more efficient than one-side roughened solar air heater. As a matter of fact, the higher efficiency of three-sides roughened duct is attributed to increase in heat transfer coefficient due to higher turbulence of air. Apart from the top absorber plate, providing roughness to both the side walls of the roughened duct in case of three-sides roughened solar air heater enhances the useful heat gain of the under flowing fluid (air) reducing absorber plate temperature that results in reduced heat loss from the roughened surface.

Hence Figures 10 and 11 represent the thermal performance of the present experimental investigations for both three-sides and one-side roughened solar air heater under varying condition of \dot{m} , p/e and e/D_h . At lower mass flow rates, the thermal efficiency of both one-side and three-sides roughened ducts increases as any of the above mentioned parameters increases. It has been found that for the present geometry used, thermal efficiency is maximum corresponding to $p/e = 12$ and $e/D_h = 0.036$ for both three-sides and one-side roughened duct. At higher mass flow rates ($\dot{m} > 0.0250$ kg/s),

there is not much difference between thermal performance of one-side and three-sides roughened duct. This is due to the fact that at higher mass flow rates, air travels quickly inside the roughened duct and it does not get sufficient time to get affected by the roughness provided inside the duct. The rise in thermal efficiency of three-sides over one-side roughened duct under varying relative roughness pitch (p/e) is found to be 44-56% and that of varying relative roughness height (e/D_h) is found to be 39-51%.

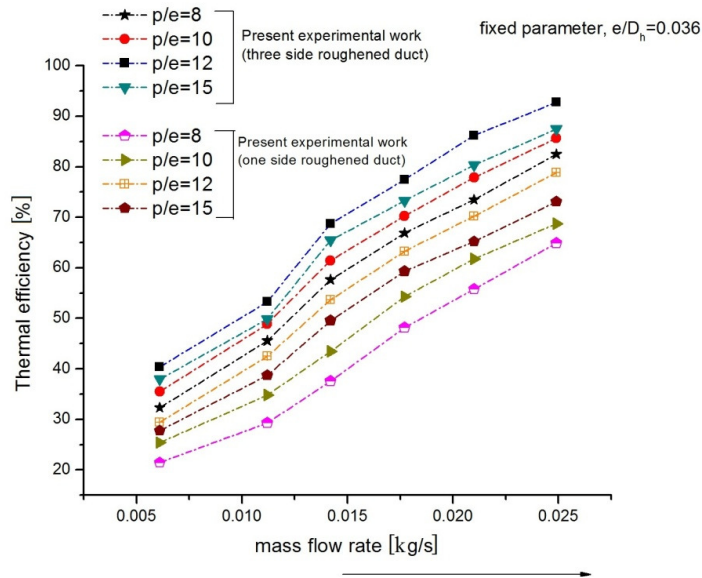


Figure 10. Thermal efficiency vs. mass flow rate at varying p/e

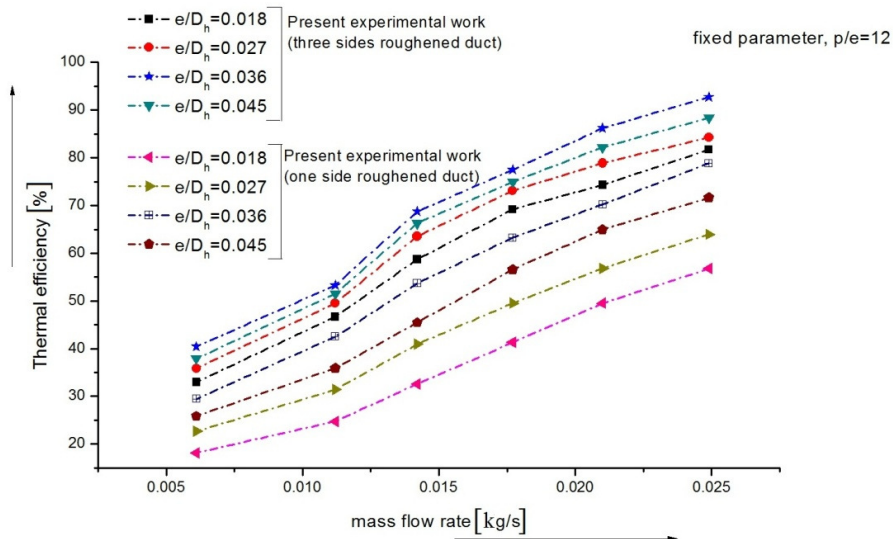


Figure 11. Thermal efficiency vs. mass flow rate at varying e/D_h

Figure 12 has been drawn to see the maximum enhancement rate in thermal performance of three-sides dimple roughened ones over those of one-side roughened ones for the range of roughness and flow parameters investigated. The augmentation in thermal efficiency due to the provision of concave dimple shape on the absorber plate is shown in Figure 12 that represents the variation of efficiency ratio $\left(\frac{\eta_{th3r}}{\eta_{th1r}}\right)$ with the mass flow rate. According to the present investigation, the maximum rise in thermal efficiency of three- sides roughened duct over one-side roughened duct is achieved corresponding to $\dot{m} = 0.015$ kg/s. Beyond this mass flow rate, the rise in efficiency is lower.

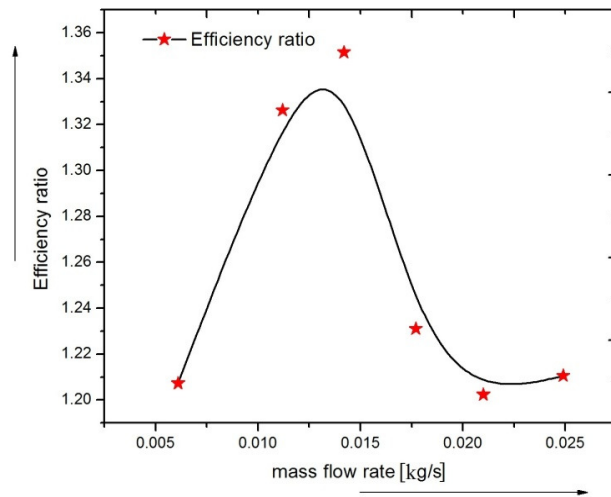


Figure 12. Efficiency ratio vs. mass flow rate

Pressure drop analysis

Artificially roughened solar air heaters are often characterized by the rise in pressure drop across the roughened duct, which results in an increment of friction co-efficient leading to a higher pumping power requirement. Numerous researchers have worked on different roughness geometry, trying to optimize the geometrical parameter to obtain a minimum rise in friction co-efficient. The effect of relative roughness pitch (p/e) and relative roughness height (e/D_h) on the friction factor with increasing mass flow rates is shown in Figures 13 and 14, respectively.

Figure 13 shows the variation in friction factor vs. mass flow rate with increasing relative roughness pitch ratio. It is evident that as the mass flow rate increases, the friction factor decreases monotonously. For both the roughened ducts, friction factor decreases with increasing relative roughness pitch. The maximum and minimum friction factor for both three sides and one side roughened ducts is obtained at the relative roughness pitch values of 8 and 15 respectively.

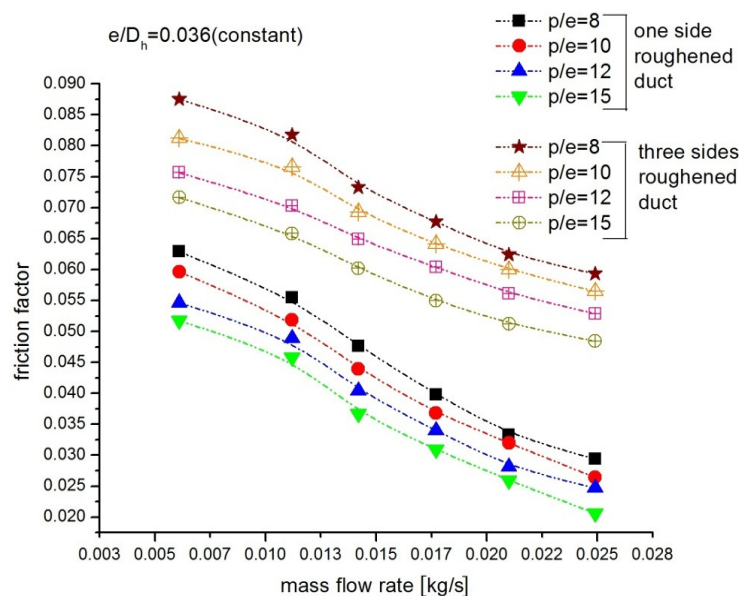


Figure 13. Effect of relative roughness pitch on ' f ' for one- and three-sides roughened duct

Figure 14 shows the variation in friction factor vs. mass flow rate with increasing relative roughness height ratio. It can be concluded that as the mass flow rate increases,

the friction factor decreases with decreasing relative roughness height. Efforts should be made to optimize the geometrical parameter to achieve maximum heat transfer rate at a minimum rise in the co-efficient of friction. The maximum and minimum friction factor for both three-sides and one-side roughened duct is obtained at relative roughness height ratio of 0.045 and 0.018, respectively.

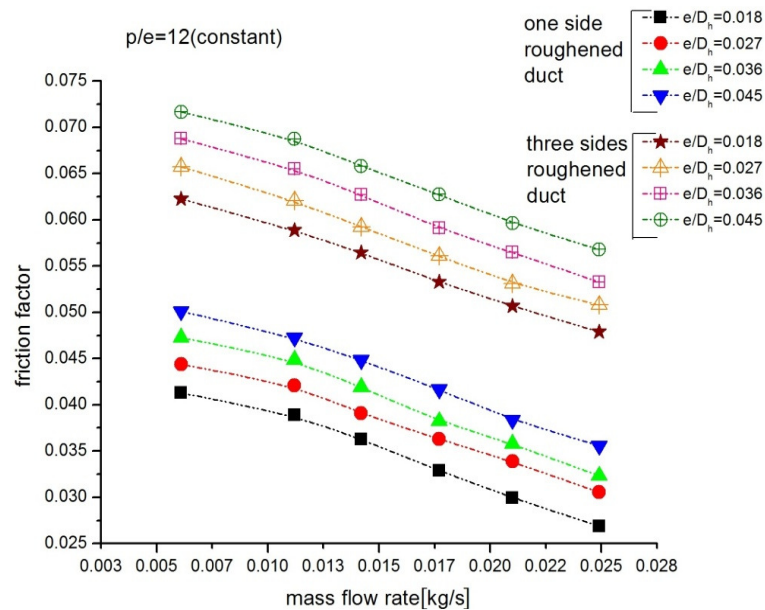


Figure 14. Effect of relative roughness height on ' f ' for one- and three-sides roughened duct

CONCLUSIONS

In the present work, experimental investigation results in terms of thermal performance for both three-sides and one-side roughened duct has been discussed. The standard mean deviation of thermal performance results for three-sides compared to one-side roughened duct is found to be $\pm 3.6\%$. The cause for such deviation has been accounted as variation in ambient condition like solar radiation, wind speed, ambient temperature, convective heat transfer coefficient, specific heat capacity of air, etc. and also uncertainty in measurements.

The augmentation in fluid temperature for three-sides compared to one-side roughened duct is found to be 34.87%. In the case of plate temperature, one-side roughened duct is at a higher temperature compared to three-sides roughened duct due to least contribution towards useful heat gain and more heat loss to the surroundings. The abatement of plate temperature in three-sides compared to one-side roughened duct is found to be 14.45%.

The plate temperature excess (mean absorber plate temperature – ambient temperature) for three-sides roughened duct is significantly lower (12.5-28.5 °C) compared to one-side roughened duct (17.5-35.5 °C) which clearly indicates that the three-sides roughened duct operates at comparatively lower temperature, hence it has a higher thermal efficiency and less heat loss from the absorber plate surface.

The augmentation in thermal efficiency due to implication of roughness in the form of concave dimple shape on the absorber plate in three-sides roughened duct is found to more than one-side roughened duct. The augmentation is found to be 44-56% for varying p/e and 39-51% for varying e/D_h . The maximum enhancement in efficiency ratio is found to be 1.35 corresponding to $\dot{m} = 0.015$ kg/s.

The augmentation in friction factor of three-sides roughened duct over one-side roughened duct for varying relative roughness pitch and relative roughness height was found to be 11-34% and 15-41%, respectively, in the range of parameters investigated.

NOMENCLATURE

A_o	area of orifice plate	$[m^2]$
A_p	area of absorber plate	$[m^2]$
C_d	coefficient of discharge	$[-]$
C_p	specific heat capacity	$[J/kgK]$
d	pipe diameter	$[m]$
D	orifice plate diameter	$[m]$
D_h	hydraulic diameter	$[m]$
e/D_h	relative roughness height	$[-]$
f	co-efficient of friction	$[-]$
g	acceleration due to gravity	$[m/s^2]$
h	heat transfer coefficient	$[W/m^2K]$
H	height of the absorber plate	$[m]$
I	insolation	$[W/m^2]$
L	length of the absorber plate	$[m]$
\dot{m}	mass flow rate	$[kg/s]$
p/e	relative roughness pitch	$[-]$
Q_u	useful heat gain	$[W]$
T_{fm}	fluid mean temperature	$[^\circ C]$
T_i	air inlet temperature	$[^\circ C]$
T_o	air outlet temperature	$[^\circ C]$
T_{pm}	plate mean temperature	$[^\circ C]$
T_∞	ambient air temperature	$[^\circ C]$
W	width of the absorber plate	$[m]$

Greek symbols

β	ratio of pipe diameter to orifice diameter	$[-]$
θ	inclination of U-tube manometer	$[^\circ]$
ρ	density	$[kg/m^3]$
η_{th}	thermal efficiency	$[%]$
ΔP	pressure drop	$[Pa]$
ΔT	temperature drop	$[^\circ C]$

Subscripts

a	air
d	duct
f	fluid
o	orifice
1r	one-side roughened
3r	three-side roughened

REFERENCES

1. Gupta, D., Solanki, S. C. and Saini, J. S., Heat and Fluid flow in rectangular Solar Air heater ducts having transverse Rib roughness on absorber Plates, *Solar Energy*, Vol. 51, No. 1, pp 31-37, 1993, [https://doi.org/10.1016/0038-092X\(93\)90039-Q](https://doi.org/10.1016/0038-092X(93)90039-Q)
2. Hans, V. S., Saini, R. P. and Saini, J. S., Performance of artificially roughened Solar Air heater – A review, *Renewable and Sustainable Energy Reviews*, Vol. 13, No. 8, pp 1854-1869, 2009, <https://doi.org/10.1016/j.rser.2009.01.030>
3. Gupta, D., Solanki, S. C. and Saini, J. S., Thermohydraulic performance of Solar Air heaters with roughened absorber Plates, *Solar Energy*, Vol. 61, No. 1, pp 33-42, 1997, [https://doi.org/10.1016/S0038-092X\(97\)00005-4](https://doi.org/10.1016/S0038-092X(97)00005-4)

4. Karwa, R., Sharma, A. and Karwa, N., A comparative Study of different roughness Geometries proposed for Solar Air heater ducts, *International Review of Mechanical Engineering (IREME)*, Vol. 4, No. 2, pp 159-66, 2010.
5. Momin, A. M. E., Saini, J. S. and Solanki, S. C., Heat transfer and friction in Solar Air heater duct with v-shaped Rib roughness on absorber Plate, *International Journal of Heat and Mass Transfer*, Vol. 45, No. 16, pp 3383-3396, 2002, [https://doi.org/10.1016/S0017-9310\(02\)00046-7](https://doi.org/10.1016/S0017-9310(02)00046-7)
6. Hans, V. S., Saini, R. P. and Saini, J. S., Heat transfer and friction Factor correlations for a Solar Air heater duct roughened artificially with multiple V-ribs, *Solar Energy*, Vol. 84, No. 6, pp 898-911, 2010, <https://doi.org/10.1016/j.solener.2010.02.004>
7. Prasad, B. N. and Saini, J. S., Effect of artificial roughness on Heat transfer and Friction Factor in a Solar Air heater, *Solar Energy*, Vol. 41, No. 6, pp 555-560, 1988, [https://doi.org/10.1016/0038-092X\(88\)90058-8](https://doi.org/10.1016/0038-092X(88)90058-8)
8. Alam, T. and Kim, M. H., A critical review on artificial roughness provided in rectangular Solar Air, *Renewable and Sustainable Energy Reviews*, Vol. 69, pp 387-400, 2017, <https://doi.org/10.1016/j.rser.2016.11.192>
9. Varun, Saini, R. P. and Singal, S. K., A review on roughness Geometry used in Solar Air heaters, *Solar Energy*, Vol. 81, No. 11, pp 1340-1350, 2007, <https://doi.org/10.1016/j.solener.2007.01.017>
10. Singh, S., Chander, S. and Saini, J. S., Investigations on Thermo-hydraulic performance due to Fow-attack-angle in V-down Rib with gap in a rectangular duct of Solar Air heater, *Applied Energy*, Vol. 97, pp 907-912, 2012, <https://doi.org/10.1016/j.apenergy.2011.11.090>
11. Karwa, R., Experimental Studies of augmented Heat transfer and friction in Asymmetrically heated rectangular ducts with Ribs on the heated Wall in Transverse, inclined, v-continuous and v-discrete Pattern, *International-Communications of Heat and Mass Transfer*, Vol. 30, No. 2, pp 241-250, 2003, [https://doi.org/10.1016/S0735-1933\(03\)00035-6](https://doi.org/10.1016/S0735-1933(03)00035-6)
12. Saini, R. P. and Saini, J. S., Heat transfer and friction Factor correlations for artificially roughened ducts with expanded Metal Mesh as roughness Element, *International Journal of Heat and Mass Transfer*, Vol. 40, No. 4, pp 973-986, 1997, [https://doi.org/10.1016/0017-9310\(96\)00019-1](https://doi.org/10.1016/0017-9310(96)00019-1)
13. Karwa, R., Bairwa, R. D., Jain, B. P. and Karwa, N., Effects of Rib angle and discretization on Heat transfer and friction in an asymmetrically heated rectangular duct, *Journal of Enhanced Heat Transfer*, Vol. 12, No. 4, pp 343-55, 2005, <https://doi.org/10.1615/JEnhHeatTransf.v12.i4.40>
14. Karwa, R., Solanki, S. C. and Saini, J. S., Heat transfer Coefficient and friction Factor correlations for the transitional Fow regime in Rib-roughened rectangular ducts, *International Journal of Heat and Mass Transfer*, Vol. 42, No. 9, pp 1597-1615, 1999, [https://doi.org/10.1016/S0017-9310\(98\)00252-X](https://doi.org/10.1016/S0017-9310(98)00252-X)
15. Karwa, R. and Chitoshiya, G., Performance Study of Solar Air heater having V-down discrete Ribs on absorber Plate, *Energy*, Vol. 55, pp 939-955, 2013, <https://doi.org/10.1016/j.energy.2013.03.068>
16. Karwa, R., Solanki, S. C. and Saini, J. S., Thermohydraulic performance of Solar Air heaters having Integral chamfered Rib roughness on absorber Plates, *Energy*, Vol. 26, No. 2, pp 161-176, 2001, [https://doi.org/10.1016/S0360-5442\(00\)00062-1](https://doi.org/10.1016/S0360-5442(00)00062-1)
17. Saini, S. K. and Saini, R. P., Development of correlations for Nusselts Number and friction Factor for Solar Air heater with roughened duct having arc-shaped Wire as artificial roughness, *Solar Energy*, Vol. 82, No. 12, pp 1118-1130, 2008, <https://doi.org/10.1016/j.solener.2008.05.010>
18. Prasad, B. N., Kumar, A. and Singh, K. D. P., Optimization of Thermo Hydraulic performance in three sides artificially roughened Solar Air heaters, *Solar Energy*, Vol. 111, pp 313-319, 2015, <https://doi.org/10.1016/j.solener.2014.10.030>

19. Bhushan, B. and Singh, R., Thermal and Thermohydraulic performance of roughened Solar Air heater having protruded absorber Plate, *Int. Journal of Solar Energy*, Vol. 86, No. 11, pp 3388-3396, 2012, <https://doi.org/10.1016/j.solener.2012.09.004>
20. Bhagoria, J. L, Saini, J. S. and Solanki, S. C., Heat transfer Coefficient and friction Factor correlations for rectangular Solar Air heater duct having transverse wedge shaped rib roughness on the absorber Plate, *Renewable Energy*, Vol. 25, No. 3, pp 341-369, 2002, [https://doi.org/10.1016/S0960-1481\(01\)00057-X](https://doi.org/10.1016/S0960-1481(01)00057-X)
21. Prasad, B. N., Behura, A. K. and Prasad, L., Fluid flow and Heat transfer analysis for Heat transfer enhancement in three sided artificially roughened Solar Air heater, *Solar Energy*, Vol. 105, pp 27-35, 2014, <https://doi.org/10.1016/j.solener.2014.03.027>
22. Behura, A. K., Prasad, B. N. and Prasad, L., Heat transfer, friction Factor and Thermal performance of three sides artificially roughened Solar Air heaters, *Solar Energy*, Vol. 130, pp 46-59, 2016, <https://doi.org/10.1016/j.solener.2016.02.006>
23. ASHRAE Standard 93-77, *Methods of testing to determine the Thermal performance of Solar Collectors*, New York, USA, 1977.
24. Hollands, K. G. T. and Shewen, E. C., Optimization of flow passage Geometry for Air heating, Plate-type Solar collectors, *Journal of Solar Energy Engineering*, Vol. 103, No. 4, pp 323-330, 1981, <https://doi.org/10.1115/1.3266260>
25. Sharma, M. and Goel, V., Performance estimation of artificially roughened Solar Air heater duct provided with continuous Ribs, *Int. Journal of Energy and Environment*, Vol. 1, No. 5, pp 897-910, 2010.
26. Kline, S. J. and McClintock, F. A., Describing uncertainties in single sample experiments, *Mechanical Engineering*, Vol. 75, pp 3-8, 1953.
27. <http://www.cwetsolar.com/index.php?option=datos&task=showfilter&estacion=31>, [Accessed: 01-March-2018]
28. Saini, R. P. and Verma, J., Heat transfer and friction correlations for a duct having dimple shape artificial roughness for Solar Air heater, *Energy*, Vol. 33, No. 8, pp 1277-1287, 2008, <https://doi.org/10.1016/j.energy.2008.02.017>

Paper submitted: 23.09.2017

Paper revised: 01.03.2018

Paper accepted: 08.04.2018